Eur. Phys. J. C 50, 823–828 (2007)
DOI 10.1140/epjc/s10052-007-0251-5

THE EUROPEAN PHYSICAL JOURNAL C

Regular Article – Theoretical Physics

# Singlet structure function $g_1$ at small $x$ and small $Q^2$

B.I. Ermolaev[1], M. Greco[2,a], S.I. Troyan[3]

[1] Ioffe Physico-Technical Institute, 194021 St. Petersburg, Russia
[2] Department of Physics and INFN, University Rome III, Via della Vasca Navale 84, 00146 Rome, Italy
[3] St. Petersburg Institute of Nuclear Physics, 188300 Gatchina, Russia

Received: 21 November 2006 / Revised version: 9 January 2007 /
Published online: 17 March 2007 – 

**Abstract.** Explicit expressions for the singlet spin structure function $g_1$ at small $x$ and small $Q^2$ are obtained with a total resummation of the leading logarithmic contributions. It is shown that $g_1$ practically does not depend on $x$ in this kinematic region. In contrast, it would be interesting to investigate its dependence on the invariant energy $2pq$, because $g_1$, being positive at small $2pq$, can turn negative at greater values of this variable. The position of the turning point is sensitive to the ratio of the initial quark and gluon densities, so its experimental detection would enable one to estimate this ratio.

**PACS.** 12.38.Cy

## 1 Introduction

The standard approach (SA) for the theoretical description of the spin structure function $g_1$ is based on the DGLAP evolution equations [1–4] complemented with global fits [5–9] for the initial parton densities. Originally, SA was suggested for describing the region of large $x$, but later it has been applied for investigating the polarized DIS at small $x$ as well. As SA neglects the total resummation of leading $\ln^k(1/x)$, which becomes necessary at small $x$, singular ($\sim x^{-\alpha}$) factors are introduced in the fits for the initial parton densities. As it was shown in [10, 11], such factors act as leading singularities[1] in Mellin space. They ensure the steep rise of $g_1$ at $x \ll 1$ and indeed mimic the impact of the total resummation of leading $\ln^k(1/x)$ terms. Alternatively, when the total resummation is taken into account, those singular factors become unnecessary, so the initial parton densities can be fitted with much simpler expressions. The total resummation of the $\ln^k(1/x)$ contributions to the anomalous dimensions and the coefficient functions of the singlet component of $g_1$ was done in [12] in the double-logarithmic (DL) approximation with the assumption of $\alpha_s$ being fixed at an unknown scale. More precise results including running $\alpha_s$ effects were obtained in [13].

In the present paper, we extend the results of [13] to consider the small-$x$ behavior of the singlet $g_1$ in more detail. In particular, we give special attention to the kinematic region where not only the $x$ but also the $Q^2$ are small. On the one hand, this kinematics has been investigated experimentally by the COMPASS Collaboration [14]. On the other hand, the region of small $Q^2$ is clearly beyond the reach of SA. We show that in this kinematics $g_1$ can be practically independent of $x$ even for $x \ll 1$. We obtain the result that $g_1$, being positive at small values of the invariant energy $2pq$, can turn negative when $2pq$ increases. The position of the turning point is sensitive to the ratio between the initial quark and gluon densities. Next, we also show that, in spite of the presence of large factors providing $g_1$ with Regge behavior at small $x$, the interplay between initial quark and gluon densities might keep $g_1$ close to zero even at small $x$, regardless of the values of $Q^2$.

The paper is organized as follows: in Sect. 2 we recall and explain the basic formulae for the singlet $g_1$ obtained in [13]. These formulae include the total resummation of the leading logarithms of $x$. In our approach, the coefficient functions for $g_1$ are expressed through new anomalous dimensions. Explicit expressions for them are presented in Sect. 3. As our approach is perturbative, we are interested in minimizing the influence of non-perturbative contributions. To this aim we introduce in Sect. 4 the optimal mass scale. We focus on $g_1$ at very small $Q^2$ in Sect. 5 and present here our numerical results based on formulae obtained in [13]. A simple and natural model for $g_1$ at small $x$ and arbitrary $Q^2$ is presented in Sect. 6. This model is based on our analysis of the Feynman graphs contributing to $g_1$. The asymptotics of $g_1$ at small $x$ and arbitrary $Q^2$ are considered in Sect. 7. Suggestions for new simple fits for the initial parton densities at arbitrary $Q^2$ are briefly discussed in Sect. 8. Finally, Sect. 9 is for our concluding remarks.

[a] e-mail: mario.greco@roma3.infn.it

[1] They are simple poles, whereas the total resummation leads to the leading singularity as the square root branch point.

## 2 Expressions for $g_1$ at small $x$ and large $Q^2$

The singlet structure function $g_1$ at small $x$ was studied in [13]. According to this reference, $g_1$ can be represented in the form of a Mellin integral:

$$g_1(x,Q^2) = \frac{\langle e_q^2 \rangle}{2} \int_{-\mathrm{i}\infty}^{\mathrm{i}\infty} \frac{\mathrm{d}\omega}{2\pi \mathrm{i}} \left(\frac{1}{x}\right)^{\omega} \times \left[ \left( C_q^{(+)} \mathrm{e}^{\Omega_{(+)} y} + C_q^{(-)} \mathrm{e}^{\Omega_{(-)} y} \right) \delta q + \left( C_g^{(+)} \mathrm{e}^{\Omega_{(+)} y} + C_g^{(-)} \mathrm{e}^{\Omega_{(-)} y} \right) \delta g \right], \quad (1)$$

where $\langle e_q^2 \rangle$ stands for the sum of the electric charges: $\langle e_q^2 \rangle = 10/9$ for $n_f = 4$, and $y = \ln(Q^2/\mu^2)$, with $\mu$ being the starting point of the $Q^2$-evolution. $\delta q$ is the initial averaged quark density: $\langle e_q^2 \rangle \delta q = e_u^2 \delta u + e_d^2 \delta d + \ldots$. whereas $\delta g$ is the initial gluon density.

The other ingredients of the integrand in (1) are expressed in terms of the anomalous dimensions $H_{ik}$, with $i,k = q,g$. The exponents $\Omega_{(\pm)}$ and coefficient functions $C_{q,g}^{(\pm)}$ are

$$\begin{aligned}
\Omega_{(\pm)} &= \frac{1}{2}\left[H_{qq} + H_{gg} \pm R\right], \quad (2)\\
C_q^{(+)} &= \frac{\omega}{RT}\Big[ \left(H_{qq} - \Omega_{(-)}\right)(\omega - H_{gg}) + H_{qg}H_{gq} + H_{gq}\left(\omega - \Omega_{(-)}\right) \Big],\\
C_q^{(-)} &= \frac{\omega}{RT}\Big[ \left(\Omega_{(+)} - H_{qq}\right)(\omega - H_{gg}) - H_{qg}H_{gq} + H_{gq}(\Omega_{(+)} - \omega) \Big],\\
C_g^{(+)} &= \frac{\omega}{RT}\Big[ \left(H_{gg} - \Omega_{(-)}\right)(\omega - H_{qq}) + H_{qg}H_{gq} + H_{qg}(\omega - \Omega_{(-)}) \Big]\left(-\frac{A'}{2\pi\omega^2}\right),\\
C_g^{(-)} &= \frac{\omega}{RT}\left[ \left(\Omega_{(+)} - H_{gg}\right)(\omega - H_{qq}) - H_{qg}H_{gq} + H_{qg}\left(\Omega_{(+)} - \omega\right) \right]\left(-\frac{A'}{2\pi\omega^2}\right). \quad (3)
\end{aligned}$$

Here

$$\begin{aligned}
R &= \sqrt{(H_{qq} - H_{gg})^2 + 4H_{qg}H_{gq}}\,,\\
T &= \omega^2 - \omega(H_{gg} + H_{qq}) + (H_{gg}H_{qq} - H_{gq}H_{qg}) \quad (4)
\end{aligned}$$

and

$$A'(\omega) = \frac{1}{b}\left[\frac{1}{\eta} - \int_0^{\infty} \frac{\mathrm{d}\rho \mathrm{e}^{-\omega\rho}}{(\rho+\eta)^2}\right], \quad (5)$$

with $\eta = \ln(\mu^2/\Lambda_{\mathrm{QCD}}^2)$ and $b = (33 - 2n_f)/(12\pi)$. The additional factor $\left(-\frac{A'}{2\pi\omega^2}\right)$ in the coefficients $C_g^{(\pm)}$ is the small-$\omega$ estimate for the quark box, which relates the initial gluons to the electromagnetic current. $A'(\omega)$ stands for the QCD coupling $\alpha_{\mathrm{s}}$ in the box in Mellin space.

## 3 Anomalous dimensions

The anomalous dimensions $H_{ik}$ obey the following system of equations:

$$\begin{aligned}
\omega H_{qq} &= b_{qq} + H_{qg}H_{gq} + H_{qq}^2,\\
\omega H_{gg} &= b_{gg} + H_{gq}H_{qg} + H_{gg}^2,\\
\omega H_{qg} &= b_{qg} + H_{qq}H_{qg} + H_{qg}H_{gg},\\
\omega H_{gq} &= b_{gq} + H_{gq}H_{qq} + H_{gg}H_{gq}\,, \quad (6)
\end{aligned}$$

where

$$b_{ik} = a_{ik} + V_{ik}\,, \quad (7)$$

with the Born contributions $a_{ik}$ defined as follows:

$$\begin{aligned}
a_{qq} &= \frac{A(\omega)C_{\mathrm{F}}}{2\pi}, \quad a_{qg} = \frac{A'(\omega)C_{\mathrm{F}}}{\pi},\\
a_{gq} &= -\frac{n_f A'(\omega)}{2\pi}, \quad a_{gg} = \frac{4NA(\omega)}{2\pi}. \quad (8)
\end{aligned}$$

$A'$ is given by (5), and

$$A(\omega) = \frac{1}{b}\left[\frac{\eta}{\eta^2+\pi^2} - \int_0^{\infty} \frac{\mathrm{d}\rho \mathrm{e}^{-\omega\rho}}{(\rho+\eta)^2+\pi^2}\right] \quad (9)$$

is the Mellin representation of the QCD running coupling $\alpha_{\mathrm{s}}$ involved in the quark–gluon ladder, with the proper account of its analytic properties. In (8) we use the standard notation for $C_{\mathrm{F}} = (N^2-1)/(2N) = 4/3$ and $N = 3$.

Finally,

$$V_{ik} = \frac{m_{ik}}{\pi^2} D(\omega)\,, \quad (10)$$

where

$$\begin{aligned}
m_{qq} &= \frac{C_{\mathrm{F}}}{2N}, \quad m_{gg} = -2N^2,\\
m_{gq} &= n_f \frac{N}{2}, \quad m_{qg} = -NC_{\mathrm{F}}\,, \quad (11)
\end{aligned}$$

and

$$D(\omega) = \frac{1}{2b^2}\int_0^{\infty} \mathrm{d}\rho \mathrm{e}^{-\omega\rho} \ln\left((\rho+\eta)/\eta\right) \times \left[\frac{\rho+\eta}{(\rho+\eta)^2+\pi^2} + \frac{1}{\rho+\eta}\right] \quad (12)$$

is the factor that accounts for non-ladder diagrams.

The solution to (6) is

$$\begin{aligned}
H_{qq} &= \frac{1}{2}\left[\omega + Z + \frac{b_{qq}-b_{gg}}{Z}\right], \quad H_{qg} = \frac{b_{qg}}{Z},\\
H_{gg} &= \frac{1}{2}\left[\omega + Z - \frac{b_{qq}-b_{gg}}{Z}\right], \quad H_{gq} = \frac{b_{gq}}{Z}, \quad (13)
\end{aligned}$$

where

$$Z = \frac{1}{\sqrt{2}}\left[(\omega^2 - 2(b_{qq}+b_{gg})) + \sqrt{(\omega^2 - 2(b_{qq}+b_{gg}))^2 - 4(b_{qq}-b_{gg})^2 - 16 b_{gq}b_{qg}}\right]^{\frac{1}{2}}. \quad (14)$$

## 4 Optimal scale for $\mu$

Besides being the starting point of the $Q^2$-evolution in (1), $\mu$ acts in our approach as a cut-off for regulating the infrared singularities in the Feynman graphs involved.[2] Introducing an infrared cut-off is unnecessary in DGLAP, because of the well-known DGLAP-ordering imposed on the transverse momenta $k_{i\perp}$ of the ladder partons:

$$\mu^2 < k_{1\perp}^2 < k_{2\perp}^2 < \cdots < k_{i\perp}^2 < \cdots < Q^2 \,, \qquad (15)$$

where $i$ numbers the ladder rungs ($i = 1, 2, \dots$) from the bottom to the top of the ladders. Equation (15) shows that $k_{i\perp}$ acts as an infrared cut-off for integrating over $k_{i+1}$. The ordering of (15) is a key-stone of DGLAP. However, as shown in [12, 13, 18, 19], this ordering, being a good approximation at $x \sim 1$, fails at small $x$. It means that regulating the infrared singularities at $x \ll 1$ should be done in every rung independently. As a result, the expression for $g_1$ in (1) depends on the cut-off $\mu$ through the parameters $y$ and $\eta$ defined in (1) and (5). Below we discuss the restrictions on the values of $\mu$. From

$$\alpha_s(k^2) = \frac{1}{b \ln(k^2/\Lambda_{\mathrm{QCD}}^2)} \,, \qquad (16)$$

as $k^2 \gg \Lambda_{\mathrm{QCD}}^2$ and $k^2 > \mu^2$, we get as a first restriction on the value of $\mu$

$$\mu \gg \Lambda_{\mathrm{QCD}} \,. \qquad (17)$$

Equation (17) guarantees the applicability of perturbative QCD as used in [13] for obtaining (1). Then the DL contributions from the ladder quark rungs are infrared-stable, with logarithms containing the masses $m_q$ of the involved quarks. In order to calculate ladder fermion graphs with our approach, one making use of infra-red evolution equations, these logs should be regulated with the infrared cut-off $\mu$. It brings about the second restriction for $\mu$:

$$\mu > m_q \,. \qquad (18)$$

Basically, there are no other restrictions for $\mu$. However, some additional information of $\mu$ comes from the small-$x$ asymptotics of $g_1$. In [13] it was shown that

$$g_1 \sim (1/x)^{\omega_0} \,, \qquad (19)$$

when $x \to 0$. It turned out that $\omega_0$ depends on $\eta = \ln(\mu^2/\Lambda_{\mathrm{QCD}}^2)$ in such a way that $\omega_0$ is maximal at $\eta = \eta_{\mathrm{S}} \approx 7.5$ with

$$\omega_0(\eta_{\mathrm{S}}) \equiv \Delta_{\mathrm{S}} \approx 0.86 \,. \qquad (20)$$

We have called $\Delta_{\mathrm{S}}$ the intercept of the singlet $g_1$. This value is in a perfect agreement with the analysis of the experimental data [17]. Assuming $\Lambda_{\mathrm{QCD}} = 0.1$ GeV leads to the estimate

$$\mu_{\mathrm{S}} = \Lambda_{\mathrm{QCD}} \mathrm{e}^{3.75} \approx 5.5 \text{ GeV} \,. \qquad (21)$$

[2] Generally, the starting point of the $Q^2$-evolution and the infrared cut-off are independent parameters.

On the other hand, the intercept $\Delta_{\mathrm{S}}$ should be a constant and should not depend on $\mu$. This dependence is an artefact of our approach: we account only for the leading part of the perturbative contribution to $\omega_0$ and leave out the possible impact of non-leading perturbative and non-perturbative contributions. Taken together, the perturbative and non-perturbative contributions would make $\omega_0$ $\mu$-independent. As soon as the leading contribution to $\omega_0$ at $\mu = \mu_{\mathrm{S}}$ proved to be in good agreement with the experimental data, all other (non-leading and non-perturbative contributions) would be minimal at that value of $\mu$. So, in order to minimize the impact of the (basically unknown) non-leading and non-perturbative contributions on $g_1$, we choose $\mu = \mu_{\mathrm{S}} = 5.5$ GeV. We call $\mu_{\mathrm{S}}$ the optimal scale for the singlet $g_1$. We expect that choosing this scale for $\mu$ would bring about better agreement between the experimental data and our formulae than other values of $\mu$. We also suggest that the initial parton densities can be fitted mostly simply when $\mu$ is fixed at the optimal scale. It is worth mentioning that in [18, 19] the optimal scale $\mu_{\mathrm{NS}}$ for the non-singlet component of $g_1$ is five times smaller: $\mu_{\mathrm{NS}} = 1$ GeV.

## 5 Numerical results for $g_1$ at small $x$ and $Q^2 \lesssim \mu^2$

In contrast to DGLAP where $Q^2$ always should be large, our approach can be applied to the region where $Q^2 \lesssim \mu^2$ [13, 18, 19]. The expression for $g_1$ in this region can be obtained from (1) by putting $y = 0$. Therefore, with the logarithmic accuracy that we keep in our approach, $g_1$ at $Q^2 \lesssim \mu^2 \ll 2pq$ depends on $z = \mu^2/(2pq)$ rather than on $x$:

$$g_1(x, z) \approx \frac{\langle e_q^2 \rangle}{2} \int_{-\mathrm{i}\infty}^{\mathrm{i}\infty} \frac{\mathrm{d}\omega}{2\pi \mathrm{i}} \left(\frac{1}{z}\right)^{\omega} \left[\omega \frac{\omega - H_{gg} + H_{gq}}{T} \delta q + \omega \frac{\omega - H_{qq} + H_{qg}}{T} \left(-\frac{A'}{2\pi\omega^2}\right) \delta g\right] . \qquad (22)$$

Presuming that $\delta q > 0$ and approximating $\delta q$ and $\delta g$ by the constants $N_{q,g}$, we rewrite (22) for $g_1$ at small $Q^2$ as

$$g_1(z) = (\langle e_q^2 \rangle / 2) N_q G_1(z) \qquad (23)$$

and calculate $G_1$ numerically. The results for different values of the ratio $r = N_g/N_q$ for $G_1$ are plotted in Fig. 1. When the gluon density is neglected, i.e. $N_g = 0$ (curve 1), $G_1$, being positive at $x \sim 1$, gets negative very soon, at $z < 0.5$, and falls fast with decreasing $z$. When $N_g/N_q = -5$ (curve 2), $G_1$ remains positive and does not grow large until $z \sim 10^{-1}$, and it turns negative at $z \sim 0.03$ and falls afterwards rapidly with decreasing $z$. This turning point where $G_1$ changes its sign is very sensitive to the magnitude of the ratio $r$. For instance, at $N_g/N_q = -8$ (curve 3), $G_1$ passes through zero at $z \sim 10^{-3}$. When $N_g/N_q < -10$, $G_1$ is positive at any values that can experimentally be reached for $z$ (curve 4). Therefore, the experimental measurement of the turning point would allow one to draw

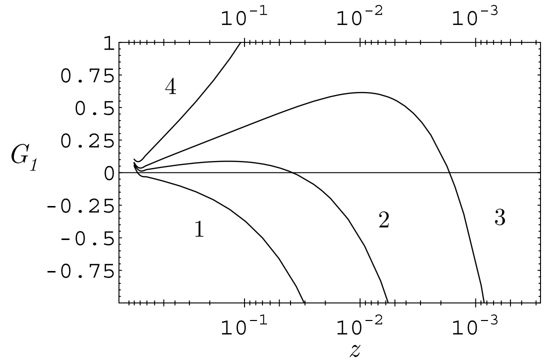


**Fig. 1.** Evolution of $G_1$ with decreasing $z = \mu^2/2(pq)$ for different values of the ratio $r = \delta g/\delta q$: *curve* 1 for $r = 0$, *curve* 2 for $r = -5$, *curve* 3 for $r = -8$ and *curve* 4 for $r = -15$

conclusions on the interplay between the initial quark and gluon densities.

## 6 A model for $g_1$ at small $x$ and small $Q^2$

Equation (1) states that, with logarithmic accuracy, $g_1$ does not depend on $Q^2$ when $Q^2 \sim \mu^2$. In this case $g_1$ is given by (22). Equation (1) was obtained for $Q^2 \gtrsim \mu^2$ and cannot be used for studying the $Q^2$-dependence of $g_1$ at $Q^2 < \mu^2$. However, it would be interesting to extend our approach to this region, even by way of a model. In order to do so, we suggest a modification of (1), replacing $Q^2$ by $(Q^2 + \mu^2)$. Although such a shift drives us out of the logarithmic accuracy we always kept in our previous papers, it looks quite reasonable and natural and can be obtained from an analysis of the Feynman graphs contributing to $g_1$. Indeed, let us in the first place consider the contribution of a ladder Feynman graph at $x \ll 1$ with the DL accuracy. This graph can include the quark and gluon rungs. Integrations of the quark rungs are infrared-stable, being regulated with the quark mass $m_q$. On the contrary, integrations of the gluon rungs are IR-divergent, so they must be regulated. The standard way of IR-regulating in QED and QCD is providing gluons with a mass $\mu$, which acts as an IR cutoff. It is also convenient to choose $\mu \gg m_q$ and replace $m_q$ by $\mu$ in the quark propagators as was first suggested in [15]. After that, $m_q$ can be dropped. Now both gluon and quark rungs of the ladder are IR-stable and $\mu$-dependent. The simplification of the spin structure can be done with the standard means (see e.g. the review [16]). It is appropriate to use the standard Sudakov variables for the integrations over the momenta $k_i$ of the virtual quarks and gluons of the ladder: $k_i = \alpha_i(p - (m_q^2/2pq)) + \beta_i(q + xp) + k_\perp$. After that, the DL contribution of a ladder graph with $n$ rungs is proportional to the integral $J_n$:

$$J_n = \int \mathrm{d}k_{n\perp}^2 \mathrm{d}\alpha_n \mathrm{d}\beta_n \times \frac{\delta(w\beta_n - Q^2 - \mu^2 + w\alpha_n\beta_n - k_{n\perp}^2)}{\alpha_n\beta_n - k_{n\perp}^2/w - \mu^2/w} \times \int \mathrm{d}k_{n-1\perp}^2 \mathrm{d}\alpha_{n-1} \mathrm{d}\beta_{n-1} \times \frac{\delta(w\alpha_n\beta_{n-1} - \mu^2 - (k_{n\perp}^2 + k_{n-1\perp}^2))}{w\alpha_{n-1}\beta_{n-1} - k_{n-1\perp}^2/w - \mu^2/w} \cdots \times \int \mathrm{d}k_{1\perp}^2 \mathrm{d}\alpha_1 \mathrm{d}\beta_1 \frac{\delta(-w\alpha_1 - \mu^2 + w\alpha_1\beta_1 - k_{1\perp}^2)}{\alpha_1\beta_1 - k_{1\perp}^2/w - \mu^2/w}, \quad (24)$$

where the rungs are numbered from the bottom to the top of the ladder. We here have used the notation $w \equiv 2pq$. As we consider $x \ll 1$, we neglected in (24) the terms $-wx\alpha_n$. They come from the representation $2qk_n = w\beta_n - wx\alpha_n$ and are present in the arguments of the $\delta$-functions. Equation (24) makes manifest that the $Q^2$-dependence in $J_n$ at $x \ll 1$ is given by the term $Q^2 + \mu^2$ in the first $\delta$-function only. Neither accounting for non-ladder graphs nor accounting for single logarithms and including running $\alpha_s$ effects change this situation. Therefore, the replacement

$$Q^2 \to \widetilde{Q}^2 \equiv Q^2 + \mu^2 \quad (25)$$

is really motivated by (24). Nevertheless, as the replacement is beyond logarithmic accuracy, it can only be treated as a model.

As it is known, DGLAP describes the $Q^2$-evolution, assuming the ordering (15), so we have the first-loop double-logarithmic contribution $J_1^{\mathrm{DGLAP}} = \ln(Q^2/\mu^2)$. This contribution is large only when $Q^2 \gg \mu^2$. The same is true for the double-logarithmic DGLAP contributions in higher loops. As the ordering fails for $x \ll 1$, we do not use it, and the integrations over $k_{i\perp}^2$ run up to $w$ instead of $Q^2$. In other words, the integrations over $k_{i\perp}^2$ in our approach are not restricted by the region of large $Q^2$. For example, when $n = 1$, (24) yields

$$J_1 = \ln(w/\mu^2), \quad (26)$$

so $J_1$ does not depend on $Q^2$ at all. The $Q^2$-dependence appears in the next loops. In particular, when $n = 2$ we have

$$J_2 = -(1/2)\ln^2(w/\mu^2)\ln\left(\widetilde{Q}^2/w\right) + (1/6)\ln^3\left(\widetilde{Q}^2/w\right), \quad (27)$$

so it depends on $Q^2$ through $Q^2 + \mu^2$. It agrees with (25). Obviously, this is also true for $J_n$ with $n > 2$. In contrast to DGLAP, double logarithms in (26) and (27) do not become small when $Q^2$ decreases.

Using the prescription (25) makes it possible to rewrite (1) in the form equally convenient for large and small $Q^2$:

$$g_1(x, Q^2) = \frac{\langle e_q^2 \rangle}{2} \times \int_{-\mathrm{i}\infty}^{\mathrm{i}\infty} \frac{\mathrm{d}\omega}{2\pi\mathrm{i}} \left(\frac{1}{z + x}\right)^{\omega} \left[\left(C_q^{(+)}(\omega)\left(\frac{Q^2 + \mu^2}{\mu^2}\right)^{\Omega_{(+)}}\right.\right.$$

$$
+C_q^{(-)}(\omega)\left(\left(\frac{Q^2+\mu^2}{\mu^2}\right)^{\Omega_{(-)}}\right)\delta q
$$
$$
-\frac{A'}{2\pi\omega^2}\left(C_g^{(+)}(\omega)\left(\frac{Q^2+\mu^2}{\mu^2}\right)^{\Omega_{(+)}}\right.
$$
$$
\left.+C_g^{(-)}(\omega)\left(\left(\frac{Q^2+\mu^2}{\mu^2}\right)^{\Omega_{(-)}}\right)\delta g\right] . \quad (28)
$$

Equation (28) can also be regarded as the formula for the interpolation between (1) and (22). Indeed, it coincides with (1) when $Q^2 \gg \mu^2$ and also reproduces (22) when $Q^2 = 0$. Equation (28) shows that the $x$- and $Q^2$-dependence of $g_1$ are getting weaker with decreasing $Q^2$, so that $g_1$ at $Q^2 \ll \mu^2$ depends on $z = \mu^2/(2pq)$ rather than on $x$ or $Q^2$. Equation (1) describes the leading $Q^2$-dependence of $g_1$ at $Q^2 \gg \mu^2$. Similarly, (28) describes the leading $Q^2$-dependence not only at large $Q^2$, but, in addition, at $Q^2 \ll \mu^2$: although the logarithms of $\left((Q^2+\mu^2)/\mu^2\right)$ are small here, they are multiplied by leading, double logarithms of $1/z$ contrary to the other $Q^2$ terms, which are beyond our control.

## 7 Small-$x$ asymptotics of $g_1$

Before making use of (28), it could be instructive to consider its small-$x$ asymptotics. This asymptotics is different for small and large $Q^2$, and when $x+z \to 0$ we obtain

$$
g_1 \sim \left(\frac{1}{x+z}\right)^{\Delta_S} \frac{K}{\ln^{3/2} 1/(x+z)} \left(\frac{Q^2+\mu^2}{\mu^2}\right)^{\Delta_S/2} \times \left(\frac{2}{\Delta_S} + \ln\frac{Q^2+\mu^2}{\mu^2}\right)\left[C_q^{\mathrm{as}}\delta q + C_g^{\mathrm{as}}\delta g\right] , \quad (29)
$$

where the intercept $\Delta_S$ is given by (20), $\Delta_S \approx 0.86$,

$$
K = \sqrt{\frac{\widetilde{\Delta_S}}{8\pi}} , \quad \widetilde{\Delta_S} = \Delta_S - \partial[(b_{gg}+b_{qq}) - r]/\partial\omega ,
$$
$$
r = \sqrt{(b_{gg}-b_{qq})^2 + 4b_{qg}b_{gq}} , \quad (30)
$$

and

$$
C_q^{\mathrm{as}} = 1 + \frac{b_{qq} - b_{gg} + 2b_{gq}}{r} ,
$$
$$
C_g^{\mathrm{as}} = \left(1 + \frac{b_{gg} - b_{qq} + 2b_{qg}}{r}\right)\left(-\frac{A'(\Delta_S)}{2\pi\Delta_S^2}\right) , \quad (31)
$$

where all $b_{ij}$ and their $\omega$-derivatives in (30) are taken at the intercept point $\omega = \Delta_S$. The initial parton densities $\delta q(\omega)$ and $\delta g(\omega)$ are also fixed at $\omega = \Delta_S$.

When $z \to 0$ and $Q^2 \ll \mu^2$, (29) turns to

$$
g_1 \sim S(\Delta_S)\delta q(\Delta_S)\left(\frac{1}{z}\right)^{\Delta_S} / \ln^{3/2}(1/z) , \quad (32)
$$

with

$$
S(\Delta_S) = -1 - 0.064\, \delta g(\Delta_S)/\delta q(\Delta_S) \quad (33)
$$

(we drop here the unessential overall factor). Equations (32)–(33) show that the asymptotics of $g_1$ does not depend on $x$ and $Q^2$ in the small-$Q^2$ region and the sign of $g_1$ is determined by $S(\Delta_S)$. We now turn to the following three options.

### 7.1 Large and negative $\delta g$: $S(\Delta_S) > 0$

When the initial gluon density is negative and large, so that

$$
\delta g < -15.64\, \delta q , \quad (34)
$$

the asymptotics of $g_1$ is positive. It is known that $g_1 > 0$ at large $z$, where it is given by its Born expression. Therefore, if $\delta q$ and $\delta g$ are related by (34), $g_1$ is positive in the whole range of $z$.

### 7.2 Positive or small and negative $\delta g$: $S(\Delta_S) < 0$

On the contrary, when

$$
\delta g > -15.64\, \delta_q , \quad (35)
$$

$g_1$, being positive at large $x$, should pass through the zero value and change sign at asymptotically small $z$.

### 7.3 Fine tuning: $S(\Delta_S) = 0$

Finally, there might be a strong correlation between $\delta q$ and $\delta g$:

$$
\delta g = 15.64 \delta q , \quad (36)
$$

when $z \to 0$. In this case $g_1$ is positive at large $x$, and then $g_1 \to 0$ in spite of the large power-like factor $(1/z)^{\Delta_S}$ in (32).

## 8 Fits for the initial parton densities

In the standard approach, the initial parton densities $\delta q(x), \delta g(x)$ are fitted by the experimental data at $x \sim 1$ and $Q^2 = \mu^2 \approx 1\,\mathrm{GeV}^2$. Then they are evolved with the anomalous dimensions into the region of large $Q^2 : Q^2 \gg \mu^2$ and finally evolved with the coefficient functions into the region of $x \ll 1$. As the coefficient functions in the SA do not include the total resummation of $\ln x$, and therefore cannot provide $g_1$ with the steep rise at small $x$, this role is assigned to the singular factors $x^{-\alpha}$ in the standard fits [5–9] that mimic the resummation. In other words, the impact of the NLO terms in the DGLAP coefficient functions on the small-$x$ behavior of $g_1$ is actually negligibly small compared to the impact of the fit. When the resummation is accounted for, the singular factors can be dropped, and the fits can be simplified down to the expressions $\sim N_{q,g}(1+c_{q,g}x)$. Obviously, the straightforward evolution of the fits backwards, to the region of $Q^2 \ll \mu^2$, is beyond the SA. We suggest that the analyses of the large $Q^2$ and small $Q^2$ experimental data would be more consistent when the argument $x$ in the new fits is replaced by $(z+x)$. This argument behaves $\approx x$ at large $Q^2$ and $\approx z$ at small $Q^2$. It means that at small $Q^2$ the fits should depend on $2pq$ only. We suggest that the fits for $\delta q(z+x), \delta g(z+x)$ can be chosen as the linear forms $N_{q,g}(1+a_{q,g}(z+x))$, where the parameters $N_{q,g}$ and $a_{q,g}$ can equally reliably be obtained from fitting by the experimental data at arbitrary $Q^2$, including $Q^2 \ll 1\,\mathrm{GeV}^2$.

## 9 Conclusion

We have shown that the study of $g_1$ at small $Q^2$ could be as interesting as in the large-$Q^2$ region. As obtained from our previous results, (22) predicts that $g_1$ at very small $Q^2$ essentially depends on $z = \mu^2/2pq$ only and practically does not depend on $x$ even at $x \ll 1$, which makes the investigation of the $x$-dependence uninteresting. On the contrary, the study of the $z$-dependence of $g_1$ at small $Q^2$ would be quite useful. Indeed, the sign of $g_1$ is positive at $z$ close to 1 and can remain positive or become negative at smaller $z$, depending on the ratio of $\delta g$ and $\delta q$. Our numerical results are plotted in Fig. 1. The position of this point is sensitive to the ratio $\delta g/\delta q$, so the experimental measurement of this point would enable one to estimate the impact of $\delta g$. In order to study the $Q^2$-dependence of $g_1$ at small $Q^2$, we suggest the simple and natural, though model-dependent, prescription (25), which allows one to obtain $g_1$ at small $x$ and arbitrary $Q^2$. This prescription follows from the analysis of the contributions (24) of the Feynman graphs at arbitrary order in $\alpha_s$. The expression for $g_1$ at small $x$ and arbitrary $Q^2$ is given by (28). Besides, the prescription (25) can be used for obtaining new fits for the initial parton densities. The fits can be defined at the scale of $Q^2 \ll 1\,\mathrm{GeV}^2$. The small-$x$ asymptotics of $g_1$ are different for large and small $Q^2$; however, both of them are of Regge type, and the intercept does not depend on $Q^2$. The sign of the asymptotics depends on the ratio between the quark and gluon initial densities. It is curious that in the case of the strong correlation (36) between them, $g_1 \to 0$ when $x \to 0$ regardless of the value of $Q^2$.

*Acknowledgements.* We are grateful to R. Windmolders, who drew our attention to the problem of describing the singlet $g_1$ in the kinematic region of small $x$ and $Q^2$. We are also grateful to G. Altarelli for useful discussions. The work is partially supported by the Russian State Grant for Scientific School RSGSS-5788.2006.2.

### Note added in proof

After this paper was finalized, the COMPASS Collaboration has presented [20] a precise measurement of the deuteron spin-dependent structure function $g_1$ at small $Q^2$ and $x$, which is found to be constant and consistent with zero in the whole kinematic range, in agreement with our predictions.

## References

1. G. Altarelli, G. Parisi, Nucl. Phys. B **126**, 297 (1977)
2. V.N. Gribov, L.N. Lipatov, Sov. J. Nucl. Phys. **15**, 438 (1972)
3. L.N. Lipatov, Sov. J. Nucl. Phys. **20**, 95 (1972)
4. Y.L. Dokshitzer, Sov. Phys. JETP **46**, 641 (1977)
5. G. Altarelli, R.D. Ball, S. Forte, G. Ridolfi, Nucl. Phys. B **496**, 337 (1997)
6. G. Altarelli, R.D. Ball, S. Forte, G. Ridolfi, Acta Phys. Pol. B **29**, 1145 (1998)
7. E. Leader, A.V. Sidorov, D.B. Stamenov, Phys. Rev. D **73**, 034 023 (2006)
8. J. Blumlein, H. Botcher, Nucl. Phys. B **636**, 225 (2002)
9. M. Hirai at al., Phys. Rev. D **69**, 054 021 (2004)
10. B.I. Ermolaev, M. Greco, S.I. Troyan, Phys. Lett. B **622**, 93 (2005)
11. B.I. Ermolaev, M. Greco, S.I. Troyan, hep-ph/0511343
12. J. Bartels, B.I. Ermolaev, M.G. Ryskin, Z. Phys. C **72**, 627 (1996)
13. B.I. Ermolaev, M. Greco, S.I. Troyan, Phys. Lett. B **579**, 321 (2004)
14. COMPASS Collaboration, E.S. Ageev et al., Phys. Lett. B **612**, 154 (2005)
15. R. Kirschner, L.N. Lipatov, Nucl. Phys. B **213**, 122 (1983)
16. V.G. Gorshkov, Usp. Fiz. Nauk. **110**, 45 (1973)
17. N.I. Kochelev, A. Lipka, W.D. Nowak, V. Vento, A.V. Vinnikov, Phys. Rev. D **67**, 074 014 (2003)
18. B.I. Ermolaev, M. Greco, S.I. Troyan, Nucl. Phys. B **571**, 137 (2000)
19. B.I. Ermolaev, M. Greco, S.I. Troyan, Nucl. Phys. B **594**, 71 (2001)
20. COMPASS Collaboration, E.S Ageev et al., hep-ex/0701014